Available online at www.sciencedirect.com
ScienceDirect
Biochimica et Biophysica Acta 1772 (2007) 473–483
Biochimica et Biophysica Acta BBA
www.elsevier.com/locate/bbadis

Cdk5 is involved in NFT-like tauopathy induced by transient cerebral ischemia in female rats

Yi Wen [a], Shao-Hua Yang [a], Ran Liu [a], Evelyn J. Perez [a], Anne Marie Brun-Zinkernagel [b], Peter Koulen [a,c], James W. Simpkins [a,c,*]

[a] Department of Pharmacology and Neuroscience, University of North Texas Health Science Center, Fort Worth, TX 76107, USA
[b] Department of Cell Biology and Genetics, University of North Texas Health Science Center, Fort Worth, TX 76107, USA
[c] Institute for Aging and Alzheimer's Disease Research, University of North Texas Health Science Center, Fort Worth, TX 76107, USA

Received 22 August 2006; received in revised form 11 October 2006; accepted 12 October 2006
Available online 18 October 2006

Abstract

Although neurofibrillary tangle (NFT) formation is a central event in both familial and sporadic Alzheimer's disease (AD), neither cellular origin nor functional consequence of the NFTs are fully understood. This largely is due to the lack of available *in vivo* models for neurofibrillary degeneration (NFD). NFTs have only been identified in transgenic mice, bearing a transgene for a rare hereditary neurodegenerative disease, frontotemporal dementia with Parkinsonism linked to chromosome 17 (FTDP17). Epidemiological evidence suggests a much higher occurrence of dementia in stroke patients. This may represent the underlying cause of the pathogenesis of sporadic AD, which accounts for the majority of AD cases. We examined pathological markers of AD in a rodent stroke model. Here we show that after transient cerebral ischemia, hyperphosphorylated tau accumulates in neurons of the cerebral cortex in the ischemic area, forms filaments similar to those present in human neurodegenerative tauopathies and colocalizes with markers of apoptosis. As a potential underlying mechanism, we were able to determine that transient ischemia induced tau hyperphosphorylation and NFT-like conformations are associated with aberrant activation of cyclin dependent kinase 5 (Cdk5) and can be rescued by delivery of a potent, but non-specific cylclin dependent kinase inhibitor, roscovitine to the brain. Our study further indicates that accumulation of p35 and its calpain-mediated cleavage product, p25 may account for the deregulation of Cdk5 induced by transient ischemia. We conclude that Cdk5 may be the principal protein kinase responsible for tau hyperphosphorylation and may be a hallmark of the tauopathies in this stroke model.

Keywords: Tauopathy; Tau; Hyperphosphorylated tau; Neurofibrillary tangle; CDK5; Roscovitine

1. Introduction

Dysfunctional and filamentous microtubule-binding tau proteins are key markers of both sporadic and familial neurodegenerative pathologies. A large number of neurodegenerative diseases, including AD, Pick's disease, progressive supranuclear palsy, corticobasal degeneration, and FTDP-17, showed progressive accumulation of dysfunctional tau inclusions [1]. Collectively, these diseases are known as neurodegenerative tauopathies. In AD, NFTs and neuropil thread pathologies are found intracellularly in conjunction with the deposition of β-amyloid (Aβ) fibrils in the extracellular space. The dominant components of neurofibrillary lesions in AD are hyperphosphorylated tau that forms paired helical filaments (PHFs) and straight filaments [2–4].

Tau proteins are microtubule-associated proteins that are expressed abundantly in axons. Both *in vivo* and *in vitro* studies indicate that tau proteins bind to microtubules, promoting their polymerization [5,6]. Multiple isoforms are expressed in the CNS by alternative mRNA splicing [7,8] and the tau isoforms observed in PHFs of AD are similar to those observed in normal adult human brain [9,10]. There are 79 potential serine and threonine phosphorylation sites on the longest human tau isoform. Phosphorylation of more than 30 of these moieties have been reported [11,12]. These phosphorylation sites are

* Corresponding author. Department of Pharmacology and Neuroscience, University of North Texas Health Science Center at Fort Worth, 3500 Camp Bowie Blvd., Fort Worth, TX 76107 2699, USA, Tel.: +1 817 735 0498.
E-mail address: JSIMPKIN@hsc.unt.edu (J.W. Simpkins).

0925-4439/$ - see front matter © 2006 Elsevier B.V. All rights reserved.
doi:10.1016/j.bbadis.2006.10.011

developmentally regulated and the degree of phosphorylation is higher in embryonic than adult CNS [13]. These phosphorylation sites cluster in the flanking region that negatively regulates tau's binding affinity to microtubules [14–16]. However, the relative importance of individual phosphorylation sites is still controversial.

A large number of Ser/Thr kinases are able to phosphorylate tau, including mitogen-activated protein kinase (MAPK) [16,17], glycogen synthase kinase 3β (GSK-3β) [18], cyclin dependent kinase 2 (cdk2) [19], cdk5 [20], cAMP dependent kinase [21], and Ca/calmodulin-dependent kinase II [22]. However, most of these protein kinases that potentially mediate tau phosphorylation were identified in *in vitro* studies, and the specific kinases that regulate tau phosphorylation under physiological or pathological conditions remain to be determined. Recent data indicate that both cdk5 and GSK3-β may be involved in the *in vivo* regulation of tauopathies [19,23–26].

The prevalence of dementia in ischemic stroke patients is nine times higher than controls at 3 months [27] and 4–12 times higher than controls at 4 years after a lacunar infarct [28]. Many of these dementias develop progressively and cerebral damage is not the direct cause of the subsequent dementia in most of the cases [29]. AD is the most prevalent dementia [30] and shares common neuropathology features with stroke. Alz-50-immunoreactive granules are found around cerebral infarction after a stroke [31], amyloid precursor protein (APP) accumulates following transient focal ischemia [32], and ApoE4 is a genetic risk factor for both AD and stroke [33].

Cdk5, also known as neuronal cdc2-like kinase, is widely expressed in many tissues [34], but its highest expression and associated kinase activity are detected only in the nervous systems [35,36]. Cdk5 shows no enzymatic activity until it associates with its co-activator, p35 or p39. One of the best-studied co-activator is p35, which can be enzymatically cleaved to p25 [37,38]. P25 contains all the elements necessary for cdk5 binding and activation. However, p25 has a substantially longer half-life than p35 and lacks the amino-terminal myristoylation site, causing it to concentrate in the cell body and nucleus, while p35 is more concentrated near the tips of neuronal processes [34]. Aberrant induction of p25 can cause extended Cdk5 activation and can redirect Cdk5 to alternative substrates to initiate apoptosis and neurodegeneration [34].

In the present study, we assessed tau-hyperphosphorylation and Alzheimer-like tangle formation in a rodent model for transient cerebral ischemia. We also examined the protein kinases that are potentially involved in the stroke-induced tauopathy.

2. Materials and methods

2.1. Animals and ovariectomy

Female Sprague–Dawley were purchased from Charles River Labs (Wilmington, MA) and maintained in pairs in temperature-controlled rooms (22–25 °C) with 12-h light–dark cycles. All rats had free access to laboratory chow and tap water. All animal procedures were reviewed and approved by the University of North Texas Health Science Center Institutional Animal Care and Use Committee, and adhered to followed current standards.

2.2. Animal surgeries

In order to avoid fluctuations of estrogens, which is neuroprotective [39,40], all animals received bilateral ovariectomy. Animals were anesthetized with ketamine (60 mg/kg) and xylazine (10 mg/kg). A small cut was made through skin and muscle, and ovaries were externalized and removed. Ovariectomies were performed at least 2 weeks before any further procedure.

For middle cerebral artery (MCA) occlusion and reperfusion, an intraluminal filament model was used [39,41]. To achieve a transient MCA occlusion, the internal carotid artery (ICA) was exposed, and a 3-0 monofilament nylon suture was introduced into the ICA lumen through a puncture and was gently advanced about 2 cm to the distal internal carotid artery (ICA) until proper resistance was felt. After 1 h, the suture was withdrawn from the ICA and the ICA was immediately cauterized. Each treatment group included 3–4 animals.

The brain was then dissected either coronally into 2-mm sections using a metallic brain matrix (ASI Instruments, Inc., Warren, MI), and stained by incubation in a 2% 2,3,5-Triphenyl-2H-tetrazolium chloride (TTC) in a 0.9% saline solution at 37 °C for 30 min. Then the slices were fixed in 4% paraformaldehyde, processed for paraffin embedding and sectioned to 5 μm for immunohistochemical analysis.

2.3. Roscovitine delivery

Rats were anesthetized and placed in a stereotaxic device. Surgical stainless steel microsyringe were temporarily inserted into the brain, so that the tip of the syringe needle would be inserted into the lateral ventricle: antero-posterior, −5; lateral, 1.8 from bregma; and −7.9 ventral from the dura. The insertion was confirmed with post-mortem dissection. Animals were administered 50 μl of 1 mM roscovitine (Sigma-Aldrich, St. Louis, WA), a potent, but non-specific cyclin dependent kinase inhibitor, in 30% 2-hydroxypropyl-β-cyclodextrin (HPβCD) into the right lateral ventricle over a period of 5 min using a microinjection syringe (equivalent to approximately 20 μM final roscovitine in the brain). The needle was held in position for at least another 30 min to avoid leaking. Sham treated animals received an equal volume of 30% HPβCD. Roscovitine was delivered at least 2 h before MCA surgery.

2.4. Immunoblotting

For immunoblotting analysis with various antibodies, frontoparietal cortex was dissected from brain tissues and homogenized in RIPA buffer (1× PBS, 1% Nonidet P-40 or Igepal CA-630, 0.5% sodium deoxycholate, 0.1% SDS, 1 mM sodium orthovanadate, 10 μg/ml Aprotinin, 100 μg/ml Phenylmethyl Sulphonyl Fluoride (PMSF)). Samples were incubated on ice for 20 min and then centrifuged at 12,000×*g* for 20 min. Supernatants were collected for further analysis. Samples were separated on 10% or 8–16% gradient SDS-polyacrylamide gels and electrophoretically transferred to a nitrocellulose membrane. Membranes were blocked by incubation with blocking buffer (5% dry milk in phosphate-buffered saline (PBS) and 0.02% Tween 20 (PBST)) for 1 h at room temperature, followed by over-night incubation at 4 °C with the appropriate primary antibody in blocking buffer. After thorough washing, the membrane was incubated with species-specific HRP-conjugated secondary antibodies for 1 h at room temperature, followed by another thorough wash in PBST. The membrane was then incubated and the blots were developed with an enhanced chemiluminescent kit (Pierce, Rockford, IL).

2.5. Immunohistochemistry and TUNEL Staining

For immunohistochemical analysis, animals were perfused transcardially with 4% paraformaldehyde in sodium phosphate buffer (pH 7.4). Brains were harvested, paraffin-embedded, and sectioned into 5 to 7 μm slices. Immunohistochemical analysis was performed using an HRP-DAB kit, following the manufacturer's recommended procedure (Zymed, South San Francisco, CA). Some of the sections were pretreated with 100 μg/ml proteinase K in PBS for 15 min for antigen retrieval, and signal enhancement. After staining, sections were dehydrated in a gradient of ethanol and xylene, and then were sealed with cover slips. All photographs were taken using a Nikon Diaphot 300 microscope and a 12-bit CCD monochrome camera, with labworks software (UVP Inc, Upland, CA).

DNA fragmentation was detected using TdT-mediated dUTP Nick-End Labeling (TUNEL) method with The DeadEnd™ Fluorometric TUNEL System (Promega, Madison, WI) according to manufacturer's instruction. Sections were counter-stained with 4′,6-diamidino-2-phenylindole, dihydrochloride (DAPI) (Molecular Probes, Eugene, OR). Colocalization of TUNEL with specific antigens was achieved by performing TUNEL in the presence of antibody, followed by the detection with highly specific Alexa-Fluorochrome conjugated secondary antibodies (Molecular Probes, Inc. Eugene, OR), whose excitation/emission spectra do not overlap with that of the FITC label, used in the TUNEL stain.

Antibodies used in the immunohistochemical assays include antibodies directed against Cdk5 (H291) and P35/P25 (C-19) at a dilution of 1:50 (Santa Cruz Biotech. Santa Cruz, CA). The following antibodies were used to label the conformation and phosphorylation dependent tau epitopes in the brain sections: MC1 (conformation dependent), TG3 (Phospho-tau 231 and AD conformation), CP13 (Phospho-tau 202/205), CP3 (Phospho-tau 214), PHF-1 (Phospho-tau 396/404), and CP9 (Phospho-tau 231) at a dilution of 1:10. All of the above-mentioned NFT specific-antibodies were characterized by and were the kind gifts of Dr. Peter Davies (Albert Einstein College of Medicine).

2.6. Sarcosyl tau extraction

Sarcosyl extractions were performed as described previously [42]. In brief, brain tissues from ischemic and contralateral rat cortex were homogenized in 10 volumes of buffer consisting of 10 mM Tris–HCl (pH 7.4), 0.8 M NaCl, 1 mM EGTA, and 10% sucrose. The homogenate was centrifuged for 20 min at 20,000×*g*. The supernatant was brought to 1% N-lauroylsarcosinate (Sarcosyl) and incubated for 1 h at room temperature with moderate shaking. Samples were then centrifuged at 100,000×*g* for 1 h at 4 °C, the sarcosyl-insoluble pellets were resuspended in 50 mM Tris–HCl (pH 7.4) and temporally stored at 4 °C, or at −80 °C for long term storage until use. This material was used for both immunoblotting analysis and electron microscopy analysis.

2.7. Electron microscopy

Resuspended sarcosyl-insoluble materials obtained from ischemic cortical or contralateral extracts were placed directly on carbon-coated, 300-mesh grids, stained with 2% phosphotungstic acid, and analyzed by electron microscopy [43]. As negative controls, filament preparations from contralateral extracts were examined at the same time. Microphotographs were recorded at an operating voltage of 80–100 kV and at nominal magnifications of 16,000 or 40,000, on a Zeiss electron microscope (Leo EM 910).

2.8. Immunocomplex protein kinase assay

For immunoprecipitation, 250 μg of brain extracts were incubated with 1 μg primary antibody at 4 °C with gentle shaking for 1 h Agarose conjugated Protein A (20 μl) was added to the tube and incubated for 1 h at 4 °C with moderate shaking. Immunoprecipitates were collected by centrifugation at 1000×*g* for 5 min at 4 °C. Pellets were washed three times with 1.0 ml lysis buffer and were resuspended with in 20 μl of the protein kinase assay buffer (e.g., 50 mM HEPES, 0.1 mM EDTA, 0.1 mg/ml BSA, 0.1% β-mercaptoethanol, 0.15 M NaCl). Histone H1 (5 μg, Upstate Waltham, MA) was added to the protein kinase assay buffer that contained a final concentration of 50 μM ATP with 1 μCi γ-^{32}P ATP (ICN Biomedicals, Inc. Irvine CA). After 15 min of reaction at 30 °C, the reaction was terminated by adding an equal volume of 2× electrophoresis sample buffer and separated on SDS-PAGE for subsequent autoradiography.

2.9. Affinity co-precipitation assay

Brain cortical extracts were incubated with recombinant tau, N-terminal 6X histidine-tagged, (Sigma, St. Louis, WA) for 1 h at 4 °C with gentle shaking, and purified with His-trap gel according to manufacturer's instruction (Amersham, Piscataway, NJ). The purified product was separated with SDS-PAGE and analyzed by immunoblotting with appropriate antibody.

2.10. Semi-quantitative cell counting

Brain sections from the rats that received roscovitine ($n=6$) or sham treatment ($n=3$) were randomly selected to estimate the density of cortical cells labeled with specific antigen, using the methods adapted from the previous studies [44]. Each brain section was labeled with specific antigen or double labeled with TUNEL immunohistochemistry. Cell counting was performed under a CAST-Grid system (Nikon, Inc) in the region selected from the ischemic brain cortex near the edge of superior surface, where the highest densities of positive cells were observed in previous studies. The striatum were not included

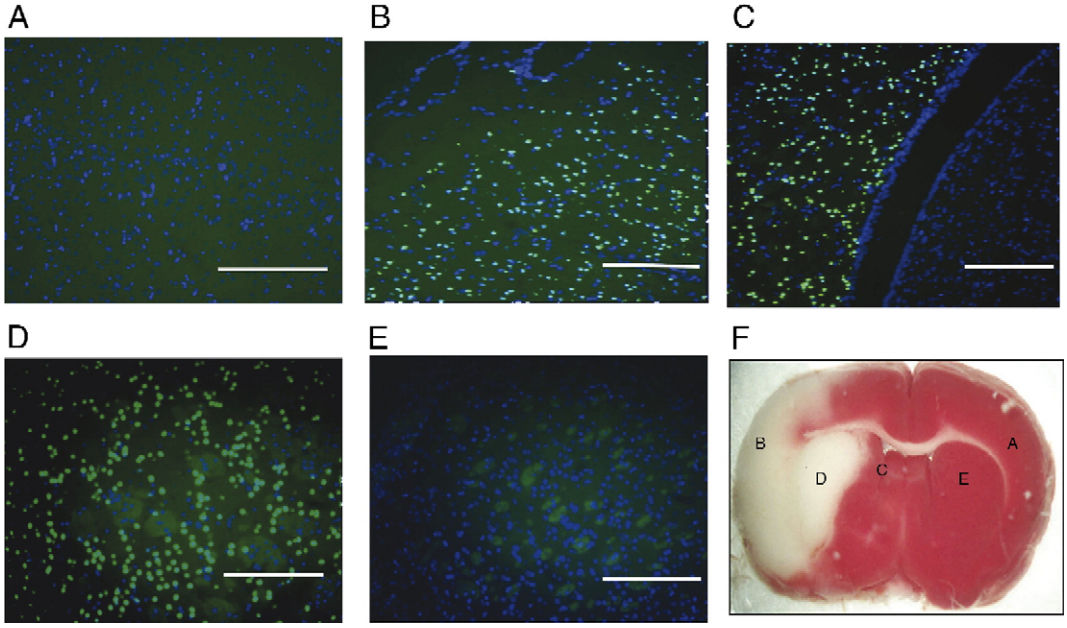

Fig. 1. Induction of apoptosis by transient cerebral ischemia in OVX rats. Depicted are TUNEL (green) stained sections from various brain regions after 1-h MCA occlusion and 24-h reperfusion with nuclear counter-stain (blue). (A) Contralateral cortex; (B) ischemic cortex; (C) periventricular region, where the ischemic region was separated from fully perfused regions by the lateral ventricle; (D) ischemic subcortex; (E) contralateral subcortex; (F) TTC stained brain slice to show the location of panels A–E. Photographs A–E were taken from the same brain section near the frontoparietal cortex in representative experiments. Scale bar=100 μm.

in this study, as few positive cells were observed in this region. Within these boundaries, optical dissectors were systematically randomly sampled, and the number of positive cells, together with DAPI labeled nuclear counter-stain in each optical dissector was counted. The cell density in the investigated region was calculated by dividing the number of positive cells counted by the total cell numbers (labeled with DAPI). The data are expressed as the percentage of DAPI counter-stained cells.

2.11. Densitometric analysis and statistical analysis

The images of autoradiography of immunoblotting were digitized and imported using a calibrated scanner, at 16-bit gray mode to provide 65,536 gray levels. The area density was quantified using Labworks software (UVP Inc, Upland, CA). The unit given is an arbitrary unit that represents the total units per band in the analyzed samples. The results were assayed with one-way ANOVA statistical method with Prism software (Version 3.0).

3. Results

3.1. Induction of neuronal apoptosis by transient cerebral ischemia

MCA occlusion in rodent is a widely used focal ischemic stroke model, at which a synchronized apoptotic process can be rapidly induced in a large number of neurons [41,45]. We examined the effects of transient MCA occlusion on neuronal apoptosis, using a TUNEL assay. As early as 2 h after the initiation of reperfusion, positive TUNEL stainings appeared in the core ischemic region near the basal ganglion areas (data not shown). At 24 h after reperfusion, TUNEL positive cells were widespread in the ischemic region, which includes fronto-parietal cerebral cortex

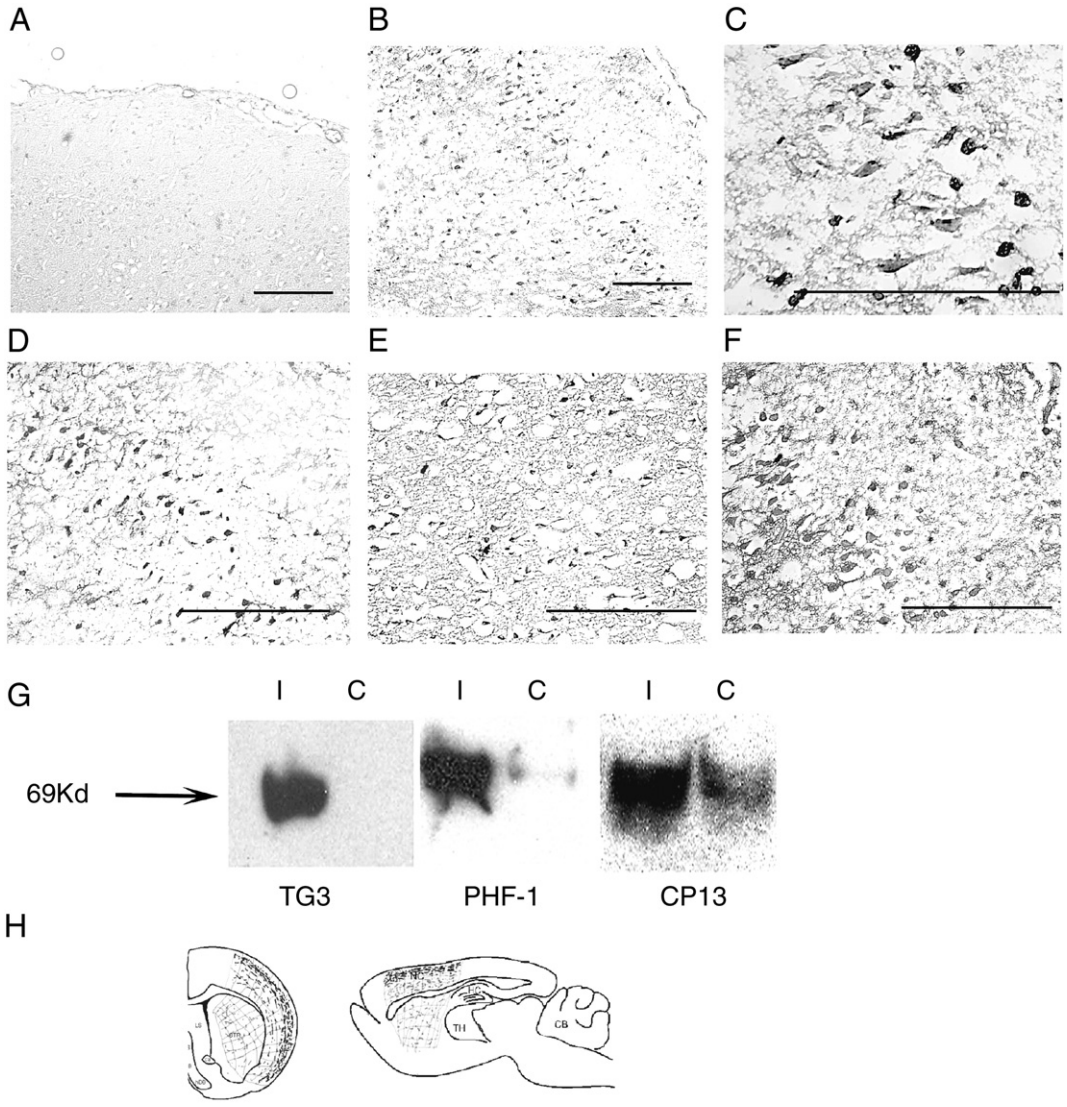

Fig. 2. Transient ischemia induces tau hyper-phosphorylation. (A–F) Representative coronal sections of frontoparietal cerebral cortex showing immunoreactivity of PHF-1 (detecting P-396/404) in the contralateral (A), ipsilateral (B), and ipsilateral in high magnification (C), CP3 (detecting P-214) (D), CP13 (detecting P-202/205), (E), and CP9 (detecting P-231) (F) in frontoparietal cortex. Scale bar = 100 μm. (G) the immunoblotting of sarcosyl extracted preparations from the ischemic (I), and contralateral (C) cortical region with specified antibody. (H) Illustration of the approximate distribution of tau-hyperphosphorylation positive neurons in coronal (left) and sagittal (right) section. The shaded area indicates the ischemic region; dotted area indicates approximate positive cell density. Most of the positive immunoreactivity is localized to the frontoparietal cerebral neocortex, with only a few immunoreactive cells present in subcortical areas. No staining was observed in non-ischemic brain regions, such as hippocampus.

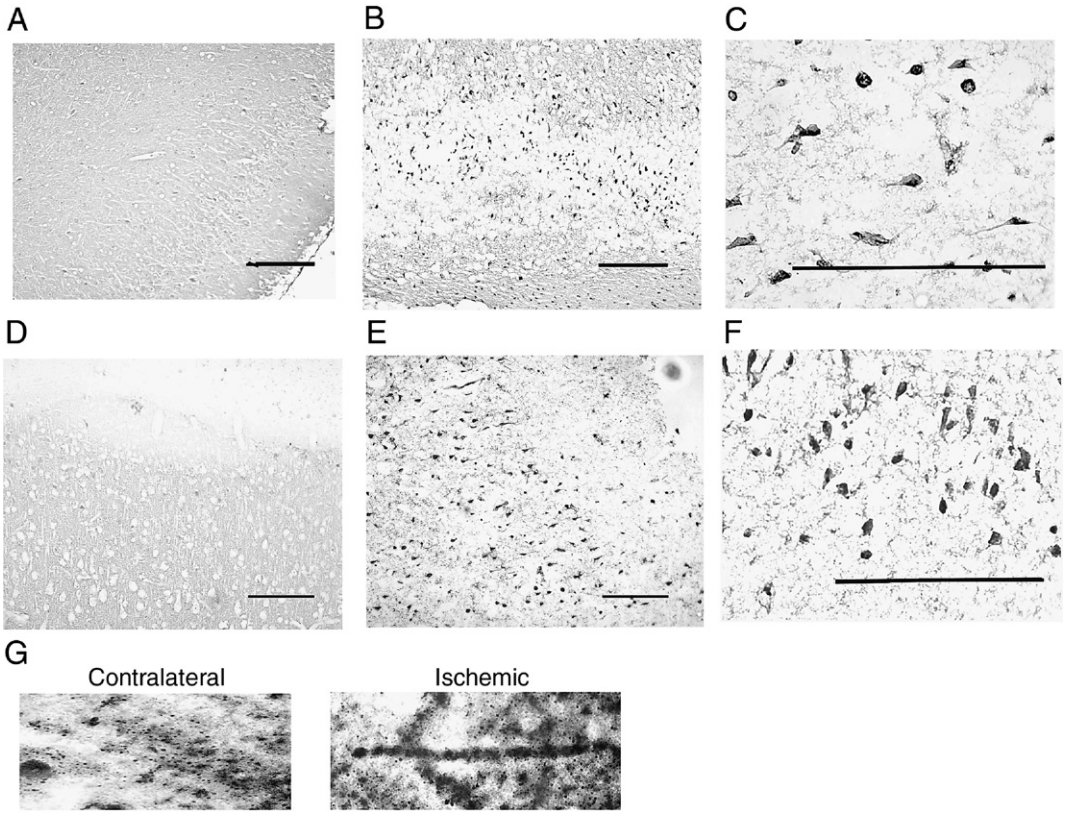

Fig. 3. Transient cerebral ischemia induces PHF-like conformation of tau protein. Tau phosphorylation and conformational changes occur 24 h after reperfusion in rats that had undergone MCA occlusion. (A–C) Antibody TG3, a phosphorylation and conformation-dependent antibody, stains a subset of pyramidal neurons of the cerebral cortical region in the ischemic region in low (B) and high (C) magnification, but not the contralateral cortex (A). (D–F) Antibody MC1, a conformation-dependent antibody, the cerebral cortical region in the ischemic region in low (E) and high (F) magnification, but not the contralateral cortex (D). (G) Electron microscopy analysis of the sarcosyl-extracted tau shows straight filaments that are approximately 20 nm wide, and resemble paired helical filaments observed in AD patients. These filaments were not observed in the contralateral extracts.

(Fig. 1B), subcortex (Fig. 1D), but were very rare in the corresponding contralateral regions (Fig. 1A, E). In the penumbra areas, where the lateral ventricle separates the ischemic from the fully perfused area, TUNEL signals were observed only on the ischemic side (Fig. 1C). In the subcortex, more than 80% of the total cell population showed positive TUNEL signals in a variety of cell types, which included neurons, astrocytes, glia, and some epithelial cells of blood vessels, as determined by morphological assessment. However in the neocortical area, most TUNEL-positive cells represent the morphology of cortical pyramidal neurons as verified by microscopic examination. The distribution of TUNEL signals was consistent with the result of TTC staining for brain slices (Fig. 1F).

3.2. Aberrant hyperphosphorylation and conformational alterations of tau in the ischemic cortical region

To characterize aberrant hyperphosphorylation of tau, we used a panel of phospho-specific antibodies. While the contralateral cortex was absent of phospho-specific immunor-

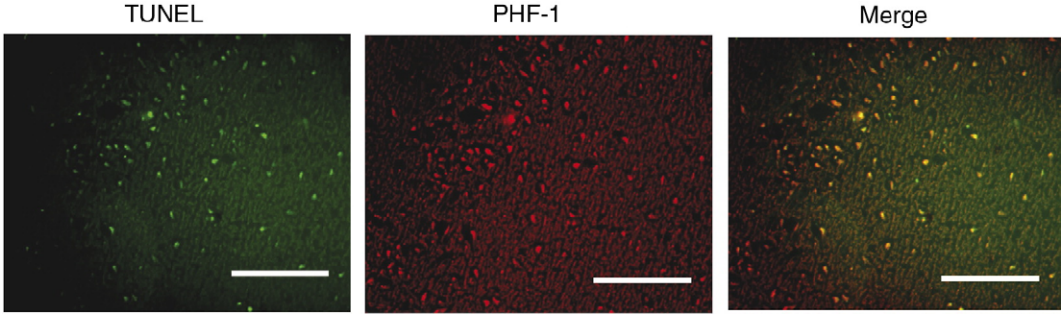

Fig. 4. Colocalization of tau hyperphosphorylation with TUNEL, a marker of late apoptotic events. In the ischemic cortical regions, PHF-1 positive staining (red) colocalized with TUNEL positive cells (green) as shown in the merged image. Scale bar = 100 μm.

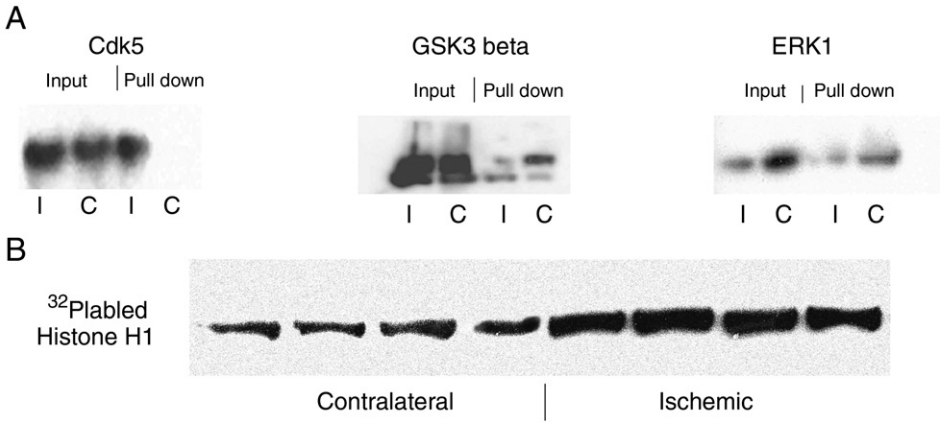

Fig. 5. Tau affinity binding assay and cdk5 activity assay. (A) Affinity binding assay of potential tau protein kinases. The contralateral and ischemic homogenate (input) was co-purified with His-tagged recombinant tau. The partially purified product (pull down) was examined using immunoblotting with the indicated antibodies. (B) Immunoprecipitation-based cdk5 kinase assay with histone H1 as substrates. Each lane represents an individual animal.

eactivity, such as PHF-1 (Fig. 2A), we observed extensive phospho-specific immunoreactivity in the ipsilateral regions, specifically for PHF-1 (Fig. 2B, C), CP3 (Fig. 2D), CP13 (Fig. 2E), and CP9 (Fig. 2F). These antibodies showed a staining pattern depicted in Fig. 2H. Briefly, most immunoreactivity was observed in the peri-infarct area of the fronto-parietal cortex. Many of positive cells can be clearly identified as pyramidal cortical neurons by morphological assessment. The subcortex lacked staining of neurons. PHF-1 and CP13 had the strongest staining for the entire soma of any given neuron, while other neurons showed only weak staining. Immunoblotting with the phospho-specific antibodies (PHF-1, CP13, and TG3) on sarcosyl-extracted cortical sample confirms the presence of hyperphosphorylation of tau protein in the sarcosyl-insoluble preparation. All three antibodies detected a band of about 69 kDa molecular weight in the sarcosyl-insoluble extracts from the ischemic cortex, but not the contralateral cortex (Fig. 2G).

To further characterize the phosphorylation and conformational status of tau in the ischemic regions, we also used two conformation-dependent anti-tau antibodies. Antibody TG3 detects both phosphorylation and the unique conformation of PHF-tau [43], while MC1 is a conformation-dependent antibody, which detects the Alz50 epitope of AD tau [46]. In the ischemic region, a large number of pyramidal neurons were immunopositive for TG3 (Fig. 3B, C) and MC1 (Fig. 3 E, F) in the frontoparietal cortex, but not in the contralateral regions (Fig. 3A, D). The staining pattern observed in TG3 and MC1 was similar to that observed with phospho-specific monoclonal antibodies (Fig. 2).

One of the major hallmarks of tauopathy is the formation of PHF-like filaments or straight filaments. To further characterize abnormal tau proteins in the ischemic region, we investigated the filamentous conformation of tau protein, using sarcosyl-insoluble preparations. In the ischemic extracts, we observed many filamentous aggregates with irregular appearance, while the contralateral extracts showed no such aggregates (Fig. 3G). A very small fraction of these filaments were similar to the paired helical filaments observed in AD brains (Fig. 3G). The filamentous conformation is consistent with that described in AD patient brains [1] and P301L transgenic mice [43]. However, filaments had a much lower density than in AD brains or the P301L animal model.

We further characterized the spatial relationship between hyperphosphorylated tau and apoptotic markers, using a double-staining method. In cortex, hyperphosphorylated tau (PHF1, red) colocalized with TUNEL (green) in a large proportion of TUNEL positive cells (Fig. 4) indicating that tau hyperphosphorylation and apoptosis are correlated events.

3.3. Activation-dependent interaction of cdk5 with tau

In order to characterize potential protein kinases responsible for the transient ischemia induced tau hyperphosphorylation, we used affinity assays with recombinant His-tagged tau as a bait protein. We examined three proline directed protein kinases, Cdk5, GSK3-β and ERK1, which had been reported to phosphorylate tau *in vitro* and *in vivo*. GSK3-β, and ERK-1 showed only weak association with recombinant tau in the affinity binding assays (Fig. 5A). However, Cdk5 showed strong association with recombinant tau in the ischemic, but not in the contralateral brain extracts (Fig. 5A). This was consistent with our previous observation that hyperphosphorylation of tau occurred only in the ischemic side. We hypothesize that the differential affinity to tau protein is related with the differential activation of Cdk5 in the ischemic and contralateral cortical regions. We used an immunocomplex protein kinase assay to evaluate Cdk5 activity. There was an induction of Cdk5 activity in the ischemic brain extracts compared with the contralateral extracts (Fig. 5B).

3.4. Deregulation of Cdk5 by its co-activator P35/P25 during transient cerebral ischemia

Cdk5 is not activated by cyclins, but by its neuronal specific co-activators, p35 or p39, as well as their cleaved product p25/

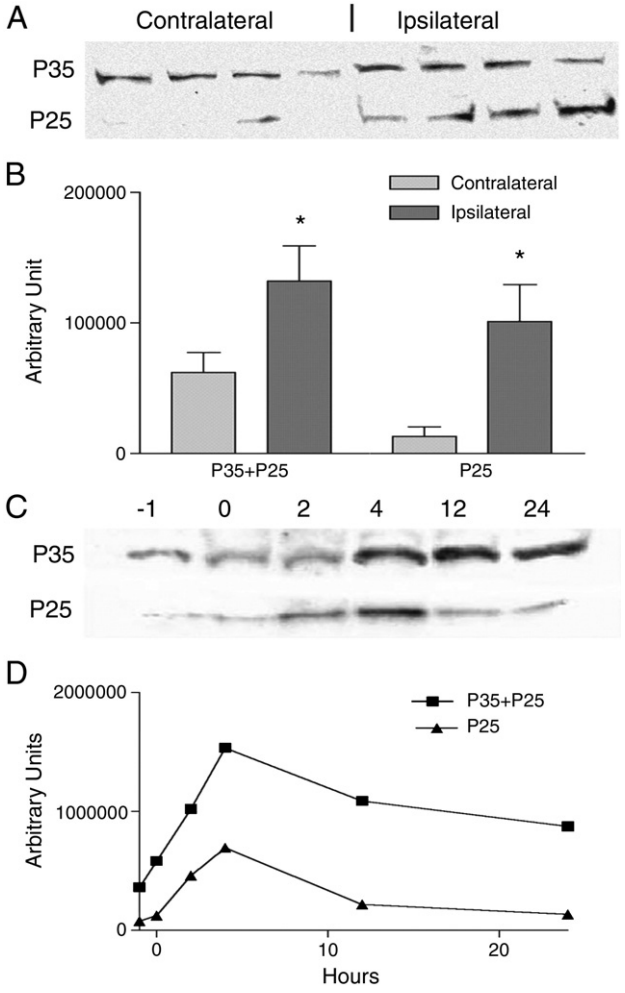

Fig. 6. Cdk5 co-activator p35/p25 in ischemic brain cortical extracts. (A) Immunoblotting analysis of p35 and p25 of contralateral (lanes 1–4) or ischemic (lanes 5–8) brain extracts. (B) Densitometric analysis of p35 cleavage in contralateral and ischemic brain extracts. (C) Immunoblotting analysis of 100 μg ipsilateral brain extracts for p35 and p25, with different time interval of reperfusion indicated by the numbers above the blot. The onset of occlusion occurred at −1 and reperfusion started at 0 h. (D) The densitometric analysis of p35 cleavage in ischemic brain cortical extracts. * indicates a statistically significant difference ($P<0.05$) between ischemic and contralateral extracts determined by Student's *t*-test.

p29 [34]. Immunoblotting of p35/p25 in brain showed a doubling in p35/p25 protein levels, and an 8-fold increase in the p25 protein levels (Fig. 6A), which is a more potent coactivator of Cdk5 and highly neurotoxic. We further analyzed the temporal pattern of p35/p25 cleavage induced by this transient cerebral ischemia *in vivo*. We found a time-dependent accumulation of p35 that lasted at least 24 h after reperfusion and a transient p25 production that started as early as 2 h and peaked at 4 h after reperfusion (Fig. 6B).

Previously published research indicated that neurotoxicity-induced calcium influx can activate calpain, a calcium dependent protease, which cleaves p35 to p25 [37]. We examined the p35 cleavage by incubating the brain cortical extract with recombinant rat calpain II. Calpain II caused a dose-dependent p35 cleavage into p25 (Fig. 7A). High concentrations of calcium caused a similar cleavage activity in brain extracts, and the calpain inhibitor, MDL 28170, attenuated this cleavage (Fig. 7B).

3.5. Inhibition of brain Cdk5 activity attenuates tau-hyperphosphorylation and NFT-like conformational epitope

In order to further confirm the relationship between this tau hyperphosphorylation and aberrant Cdk5 activation, we delivered roscovitine, a potent but non-specific cyclin-dependent kinase inhibitor (K_i=0.7 μM), in the lateral ventricle. The effect of this treatment was evaluated by both examining the phospho-epitopes with TG3 labeling (Fig. 8A), by immunoblotting analysis of the brain cortical extract, and by semi-quantitative cell counting in the ischemic cortex. Roscovitine treatment reduced the number of TG3 epitope positive cells from an average of 17.4±0.79% in sham treated animals to an average of 6.5±0.78% in roscovitine treated animals (Fig. 8B). Immunoblotting of brain cortical extracts with monoclonal antibodies, which recognize the phosphorylated tau, revealed multiple bands ranging from 31 kDa to 69 kDa. This observation is consistent with previous research that has identified tau protein isoforms in rodents [47]. Roscovitine treatment caused a reduction of tau hyperphosphorylation epitopes in the ischemic cortical extract (Fig. 8C).

4. Discussion

This study shows that transient cerebral ischemia leads to the hyperphosphorylation of tau protein and induces PHF-like tau conformations in wild type female rats. Transgenic mice that bear mutations of tau have been described for filamentous tau aggregation [20,43]. However, these mutations in tau protein are not related to AD, but to a rare neurodegenerative disease, FTDP17 [48]. Another drawback of mice bearing tau mutations is that they are not under control of an endogenous tau promoter, but a much stronger promoter, Thy 1.2 [20,43] that may affect tau distribution and signal regulation. In the present study, we demonstrated that transient ischemia causes neuronal loss and

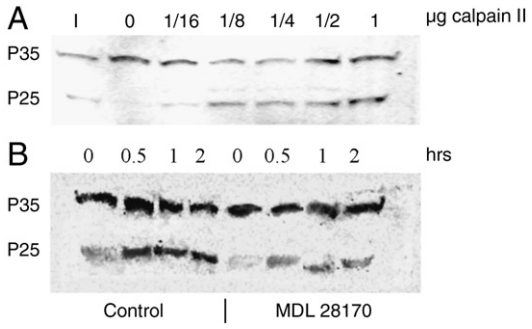

Fig. 7. Calpain activation is involved in p35 cleavage and Cdk5 activation induced by transient ischemia. (A) Immunoblotting analysis of p35 cleavage with recombinant rat calpain II. The first lane was loaded with 25 μg ischemic brain extracts; other lanes are 100 μg contralateral brain extracts incubated with the indicated amount of recombinant calpain II for 60 min at 37 °C. (B) Immunoblotting analysis of p35/p25 in the cortical brain extract incubated with 5 mM calcium in the presence (lanes 5–8) or absence (lanes 1–4) of a calpain inhibitor (MDL 28170) for 4 h at 37 °C.

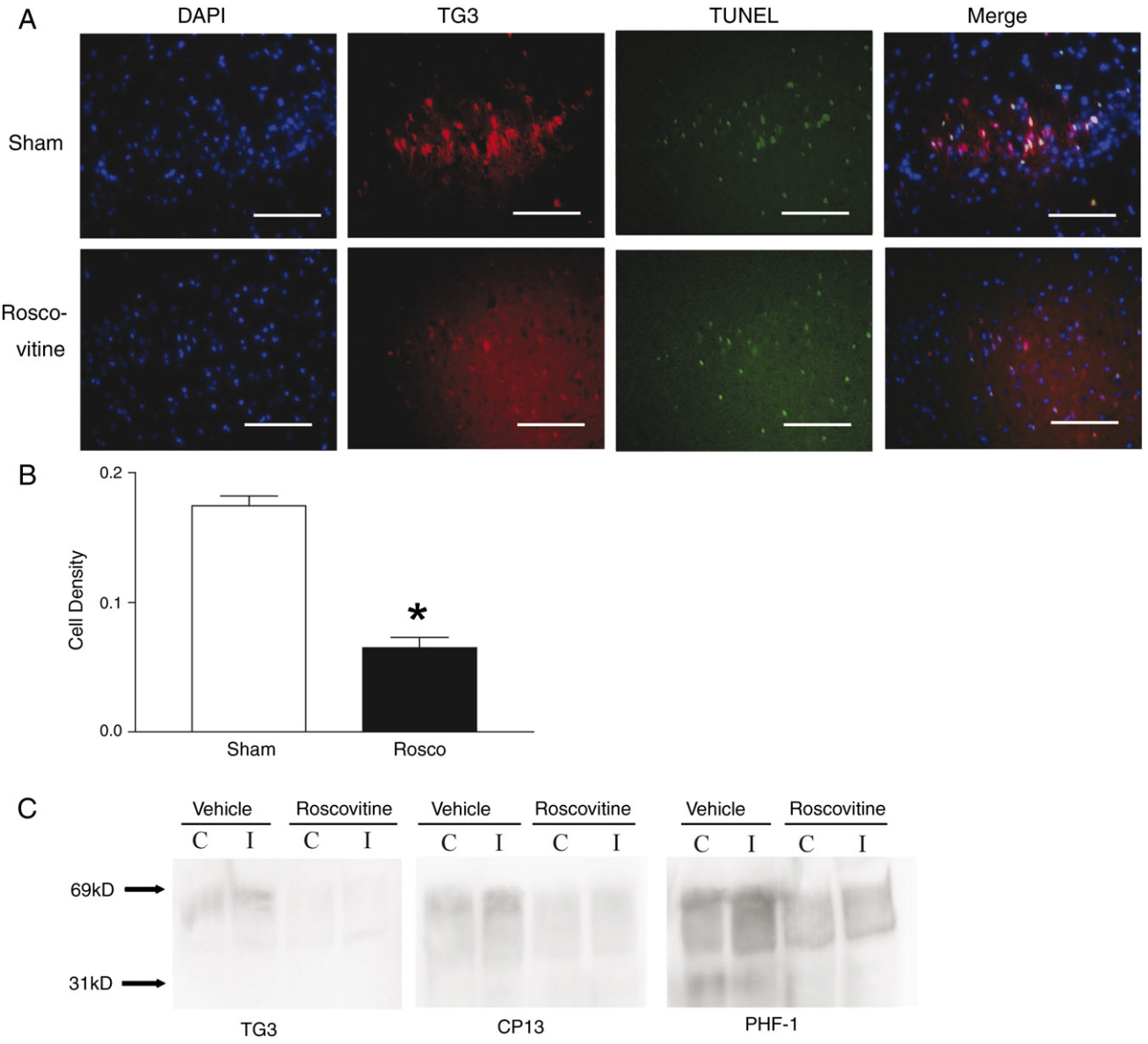

Fig. 8. Inhibition of cyclin dependent kinases reduces tau hyperphosphorylation and tauopathy conformation. (A) Representative immunofluorescent staining of TG3 in sham (upper panel) and roscovitine treated (lower panel) brains after transient cerebral ischemia in the ischemic cortex. Blue indicates nuclear counterstaining with DAPI, red indicates phospho-tau epitope, TG3 staining, green indicates apoptosis marker TUNEL. Scale bar = 100 μm (B) Semi-quantitative analysis on the effects of roscovitine injection on TG3 immunostaining cell density, in percentage of total cell numbers in frontoparietal cortex. (C) Representative immunoblotting of cortical extracts with indicated monoclonal antibodies. I: ipsilateral, C: contralateral.

tauopathies in rodents without genetic alterations. We further investigated the potential tau kinases and determined that aberrant Cdk5 activation is involved in this transient ischemia induced tau hyperphosphorylation.

These findings are consistent with epidemiological studies that show that the prevalence of dementia in ischemic stroke patients is higher than in control subjects [27,28]. This suggests that NFT formation may be a consequence of a preceding apoptotic event, which results in the aberrant activation of protein kinases and further causes tau hyperphosphorylation and tangle formation. Multiple studies support the conclusion that the apoptotic signaling pathways are involved in neuronal loss in AD brains [49–51]. A number of pro-apoptotic factors, including reactive oxygen species [52,53], β-amyloid [54] and growth factor reduction [55,56] may serve as the initiator of neurodegenerative diseases. Tau hyperphosphorylation and tangle formation is associated with apoptosis in AD patients [57–59] and can be induced or enhanced by amyloidal deposits [42,60].

Our findings that aberrant Cdk5 activation is involved in transient ischemia induced tauopathy, support the hypothesis that Cdk5 is involved in AD pathogenesis and NFT formation. Tau protein kinases II (TPKII), which was purified from bovine brain microtubules was shown to be identical to the p25–Cdk5 complex [61]. In the human brain, conversion from p35 to p25 is strongly correlated with AD [38,62] and both Cdk5 and p25 are present in neurons that contain NFTs [63]. Cdk5 is associated with NFTs *in vivo* and phosphorylates tau on sites

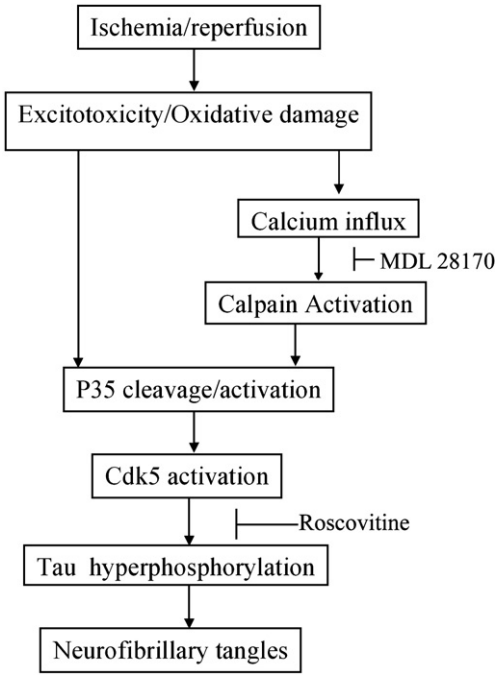

Fig. 9. Proposed model for induction of NFTs by cerebral ischemia/reperfusion damage.

found in PHF-tau [64]. Compared with p35, p25 has a substantially longer half-life and is considered neurotoxic. The generation of p25 is, therefore, likely to disrupt the normal regulation of Cdk5, directing Cdk5 to alternate substrates, causing neurite retraction, microtubule collapse and apoptosis [38]. P35 cleavage can be induced by calcium influx and activation of calpain, a calcium-dependent protease [37]. P35–Cdk5 poorly phosphorylates tau, whereas p25–Cdk5 can potently induce tau phosphorylation [65]. Cdk5 is also involved in amyloid induced toxicity [66,67]. In the present study, Cdk5 appears to be involved in tau hyperphosphorylation *in vivo*. Cdk5 is strongly activated by the transient cerebral ischemia and directly associates with tau in an activation-dependent manner in our study. In contrast, GSK3-β does not appear to be involved in the initiation of tau-hyperphosphorylation in our model. During this ischemia–reperfusion process, GSK3-β is inactivated by the activation of Akt signaling pathways (data not shown) and is not likely to account for the tau hyperphosphorylation observed in ischemic brains. However, following the cdk5 induced initial phosphorylation of critical amino acid residues, GSK3-β may further phosphorylate tau protein and further negatively regulates its binding to microtubules.

The MCA occlusion model has been widely used for the evaluation of neurodegenerative mechanisms in stroke and neuroprotective compounds, such as estrogen [39,68–70]. Our results indicate that this transient ischemic model may be used for evaluating tau hyperphosphorylation and NFT-conformation *in vivo*, as well as for pharmaceutical screening for NFTs inhibitors *in vivo*. Finally, the present data also suggest that sporadic hypo-perfusion of the brain may initiate and contribute to the progression of neuropathology in non-familial AD patients and provides mechanism of the long-observed correlation between the ischemic events and the increased prevalence of AD [28]. As such, prevention of ischemic episodes may serve as an additional therapeutic approach to prevent the initiation and progression of AD.

Collectively, our data support the proposed model for NFT-like tauopathy induced by ischemia/reperfusion shown in Fig. 9. Ischemia/reperfusion causes a variety of pro-apoptotic processes, including energy depletion, excitotoxicity, and oxidative damage [71,72]. These neurotoxic events lead to disturbances in cellular Ca^{2+} homeostasis and results in elevated calpain activity. Activated calpain cleaves p35 to p25, which confers potent neurotoxicity in neurons and may lead to sustained deregulation of Cdk5 in neurons [37,62,73]. The resulting alteration in kinase activities ultimately leads to the hyperphosphorylation of tau and potentially the formation of neurofibrillary tangles [74]. The above process is consistent with the amyloid hypothesis in AD, which proposes that amyloid beta peptides disrupt neuronal metabolic and ionic homeostasis and cause aberrant calcium homeostasis, as well as activation of kinases and/or inhibition of phosphatases. The resulting alteration in kinase/phosphatase activities leads to hyperphosphorylation of tau and formation of neurofibrillary tangles [74]. Our results suggest that cdk5 may be the mediator, which bridges amyloid toxicity and neurofibrillary tangle formation.

The present study indicates that the transient cerebral ischemia can induce tau-hyperphosphorylation and potential NFT formation in a rodent model without genetic alteration. This could provide valuable information about the pathogenesis and signal transduction pathways involved in the neurodegenerative diseases. Our results also suggest aberrant Cdk5 activation is involved in the tau-hyperphosphorylation in this animal model and may be a good therapeutic target for the developments of anti-tangle therapy strategies in AD treatments. Finally, these results suggest that therapies directed at preventing the early stage of apoptosis may be able to prevent subsequent neuropathological events seen in AD.

Acknowledgements

This study was supported by grants AG010485 and AG022550 from NIH/NIA (JWS and PK) and a New Investigator grant NIRG-03-6161 from the Alzheimer's Association (PK).

References

[1] V.M. Lee, M. Goedert, J.Q. Trojanowski, Neurodegenerative tauopathies, Annu. Rev. Neurosci. 24 (2001) 1121–1159.
[2] J. Kondo, T. Honda, H. Mori, Y. Hamada, R. Miura, M. Ogawara, Y. Ihara, The carboxyl third of tau is tightly bound to paired helical filaments, Neuron 1 (1988) 827–834.
[3] K.S. Kosik, L.D. Orecchio, L. Binder, J.Q. Trojanowski, V.M. Lee, G. Lee, Epitopes that span the tau molecule are shared with paired helical filaments, Neuron 1 (1988) 817–825.
[4] V.M. Lee, B.J. Balin, L. Otvos Jr., J.Q. Trojanowski. A68: a major subunit of paired helical filaments and derivatized forms of normal Tau Science 251 (1991) 675–678.
[5] M.D. Weingarten, A.H. Lockwood, S.Y. Hwo, M.W. Kirschner, A protein

factor essential for microtubule assembly, Proc. Natl. Acad. Sci. U. S. A. 72 (1975) 1858–1862.
[6] D.W. Cleveland, S.Y. Hwo, M.W. Kirschner, Purification of tau, a microtubule-associated protein that induces assembly of microtubules from purified tubulin, J. Mol. Biol. 116 (1977) 207–225.
[7] R.L. Neve, P. Harris, K.S. Kosik, D.M. Kurnit, T.A. Donlon, Identification of cDNA clones for the human microtubule-associated protein tau and chromosomal localization of the genes for tau and microtubule-associated protein 2, Brain Res. 387 (1986) 271–280.
[8] M. Goedert, C.M. Wischik, R.A. Crowther, J.E. Walker, A. Klug, Cloning and sequencing of the cDNA encoding a core protein of the paired helical filament of Alzheimer disease: identification as the microtubule-associated protein tau, Proc. Natl. Acad. Sci. U. S. A. 85 (1988) 4051–4055.
[9] J.Q. Trojanowski, V.M. Lee, Paired helical filament tau in Alzheimer's disease. The kinase connection, Am. J. Pathol. 144 (1994) 449–453.
[10] M. Goedert, R. Jakes, M.G. Spillantini, R.A. Crowther, P. Cohen, E. Vanmechelen, A. Probst, J. Gotz, K. Burki, Tau protein in Alzheimer's disease, Biochem. Soc. Trans. 23 (1995) 80–85.
[11] M.L. Billingsley, R.L. Kincaid, Regulated phosphorylation and dephosphorylation of tau protein: effects on microtubule interaction, intracellular trafficking and neurodegeneration, Biochem. J. 323 (1997) 577–591.
[12] L. Buee, T. Bussiere, V. Buee-Scherrer, A. Delacourte, P.R. Hof, Tau protein isoforms, phosphorylation and role in neurodegenerative disorders, Brain Res. Brain Res. Rev. 33 (2000) 95–130.
[13] K. Kanemaru, T. K.akio, R. Miura, K. Titani, Y. Ihara, Fetal-type phosphorylation of the tau in paired helical filaments, J. Neurochem. 58 (1992) 1667–1675.
[14] J. Biernat, N. Gustke, G. Drewes, E.M. Mandelkow, E. Mandelkow, Phosphorylation of Ser262 strongly reduces binding of tau to microtubules: distinction between PHF-like immunoreactivity and microtubule binding, Neuron 11 (1993) 153–163.
[15] G.T. Bramblett, M. Goedert, R. Jakes, S.E. Merrick, J.Q. Trojanowski, V.M. Lee, Abnormal tau phosphorylation at Ser396 in Alzheimer's disease recapitulates development and contributes to reduced microtubule binding, Neuron 10 (1993) 1089–1099.
[16] D.N. Drechsel, A.A. Hyman, M.H. Cobb, M.W. Kirschner, Modulation of the dynamic instability of tubulin assembly by the microtubule-associated protein tau, Mol. Biol. Cell 3 (1992) 1141–1154.
[17] G. Drewes, B. Lichtenberg-Kraag, F. Doring, E.M. Mandelkow, J. Biernat, J. Goris, M. Doree, E. Mandelkow, Mitogen activated protein (MAP) kinase transforms tau protein into an Alzheimer-like state, EMBO J. 11 (1992) 2131–2138.
[18] D.P. Hanger, K. Hughes, J.R. Woodgett, J.P. Brion, B.H. Anderton, Glycogen synthase kinase-3 induces Alzheimer's disease-like phosphorylation of tau: generation of paired helical filament epitopes and neuronal localisation of the kinase, Neurosci. Lett. 147 (1992) 58–62.
[19] K. Baumann, E.M. Mandelkow, J. Biernat, H. Piwnica-Worms, E. Mandelkow, Abnormal Alzheimer-like phosphorylation of tau-protein by cyclin-dependent kinases cdk2 and cdk5, FEBS Lett. 336 (1993) 417–424.
[20] B. Allen, E. Ingram, M. Takao, M.J. Smith, R. Jakes, K. Virdee, H. Yoshida, M. Holzer, M. Craxton, P.C. Emson, et al., Abundant tau filaments and nonapoptotic neurodegeneration in transgenic mice expressing human P301S tau protein, J. Neurosci. 22 (2002) 9340–9351.
[21] J.M. Litersky, G.V. Johnson, Phosphorylation by cAMP-dependent protein kinase inhibits the degradation of tau by calpain, J. Biol. Chem. 267 (1992) 1563–1568.
[22] J. Baudier, R.D. Cole, Phosphorylation of tau proteins to a state like that in Alzheimer's brain is catalyzed by a calcium/calmodulin-dependent kinase and modulated by phospholipids, J. Biol. Chem. 262 (1987) 17577–17583.
[23] T.J. Singh, N. Haque, I. Grundke-Iqbal, K. Iqbal, Rapid Alzheimer-like phosphorylation of tau by the synergistic actions of non-proline-dependent protein kinases and GSK-3, FEBS Lett. 358 (1995) 267–272.
[24] M. Hong, D.C. Chen, P.S. Klein, V.M. Lee, Lithium reduces tau phosphorylation by inhibition of glycogen synthase kinase-3, J. Biol. Chem. 272 (1997) 25326–25332.
[25] S. Lovestone, D.R. Davis, M.T. Webster, S. Kaech, J.P. Brion, A. Matus, B.H. Anderton, Lithium reduces tau phosphorylation: effects in living cells and in neurons at therapeutic concentrations, Biol. Psychiatry 45 (1999) 995–1003.
[26] J. Lew, Q.Q. Huang, Z. Qi, R.J. Winkfein, R. Aebersold, T. Hunt, J.H. Wang, A brain-specific activator of cyclin-dependent kinase 5, Nature 371 (1994) 423–426.
[27] T.K. Tatemichi, D.W. Desmond, R. Mayeux, M. Paik, Y. Stern, M. Sano, R.H. Remien, J.B. Williams, J.P. Mohr, W.A. Hauser, et al., Dementia after stroke: baseline frequency, risks, and clinical features in a hospitalized cohort, Neurology 42 (1992) 1185–1193.
[28] C. Loeb, C. Gandolfo, R. Croce, M. Conti, Dementia associated with lacunar infarction, Stroke 23 (1992) 1225–1229.
[29] T.K. Tatemichi, M. Paik, E. Bagiella, D.W. Desmond, Y. Stern, M. Sano, W.A. Hauser, R. Mayeux, Risk of dementia after stroke in a hospitalized cohort: results of a longitudinal study, Neurology 44 (1994) 1885–1891.
[30] F. Pasquier, D. Leys, Why are stroke patients prone to develop dementia? J. Neurol. 244 (1997) 135–142.
[31] K. Ikeda, H. Akiyama, T. Arai, H. Kondo, C. Haga, K. Tsuchiya, S. Yamada, S. Murayama, A. Hori, Neurons containing Alz-50-immunoreactive granules around the cerebral infarction: evidence for the lysosomal degradation of altered tau in human brain? Neurosci. Lett. 284 (2000) 187–189.
[32] J. Shi, S.H. Yang, L. Stubley, A.L. Day, J.W. Simpkins, Hypoperfusion induces overexpression of beta-amyloid precursor protein mRNA in a focal ischemic rodent model, Brain Res. 85 (2000) 1–4.
[33] J.H. Contois, D.E. Anamani, G.J. Tsongalis, The underlying molecular mechanism of apolipoprotein E polymorphism: relationships to lipid disorders, cardiovascular disease, and Alzheimer's disease, Clin. Lab. Med. 16 (1996) 105–123.
[34] R. Dhavan, L.H. Tsai, A decade of CDK5, Nat. Rev., Mol. Cell Biol. 2 (2001) 749–759.
[35] M.R. Hellmich, H.C. Pant, E. Wada, J.F. Battey, Neuronal cdc2-like kinase: a cdc2-related protein kinase with predominantly neuronal expression, Proc. Natl. Acad. Sci. U. S. A. 89 (1992) 10867–10871.
[36] L.H. Tsai, T. Takahashi, V.S. Caviness Jr., E. Harlow, Activity and expression pattern of cyclin-dependent kinase 5 in the embryonic mouse nervous system, Development 119 (1993) 1029–1040.
[37] M.S. Lee, Y.T. Kwon, M. Li, J. Peng, FR. M.riedlander, L.H. Tsai, Neurotoxicity induces cleavage of p35 to p25 by calpain, Nature 405 (2000) 360–364.
[38] G.N. Patrick, L. Zukerberg, M. Nikolic, S. de la Monte, P. Dikkes, L.H. Tsai, Conversion of p35 to p25 deregulates Cdk5 activity and promotes neurodegeneration, Nature 402 (1999) 615–622.
[39] J.W. Simpkins, G. Rajakumar, Y.Q. Zhang, C.E. Simpkins, D. Greenwald, C.J. Yu, N. Bodor, A.L. Day, Estrogens may reduce mortality and ischemic damage caused by middle cerebral artery occlusion in the female rat, J. Neurosurg. 87 (1997) 724–730.
[40] W.P. M.ise, D.B. Dubal, M.E. Wilson, S.W. Rau, M. Bottner, Minireview: neuroprotective effects of estrogen—New insights into mechanisms of action, Endocrinology 142 (2001) 969–973.
[41] A.M. Bremer, O. Watanabe, R.S. Bourke, Artificial embolization of the middle cerebral artery in primates. Description of an experimental model with extracranial technique, Stroke 6 (1975) 387–390.
[42] J. Gotz, F. Chen, J. van Dorpe, R.M. Nitsch, Formation of neurofibrillary tangles in P301l tau transgenic mice induced by Abeta 42 fibrils, Science 293 (2001) 1491–1495.
[43] J. Gotz, F. Chen, R. Barmettler, R.M. Nitsch, Tau filament formation in transgenic mice expressing P301L tau, J. Biol. Chem. 276 (2001) 529–534.
[44] W. Jiang, W. Gu, T. Brannstrom, R. Rosqvist, P. Wester, Cortical neurogenesis in adult rats after transient middle cerebral artery occlusion, Stroke 32 (2001) 1201–1207.
[45] Y. Li, M. Chopp, C. Powers, N. Jiang, Apoptosis and protein expression after focal cerebral ischemia in rat, Brain Res. 765 (1997) 301–312.
[46] G.A. Jicha, R. Bowser, I.G. Kazam, P. Davies, Alz-50 and MC-1, a new monoclonal antibody raised to paired helical filaments, recognize conformational epitopes on recombinant tau, J. Neurosci. Res. 48 (1997) 128–132.
[47] H. Takuma, S. Arawaka, H. Mori, Isoforms changes of tau protein during

development in various species, Brain Res. Dev. Brain Res. 142 (2003) 121–127.
[48] G.V. Johnson, C.D. Bailey, Tau, where are we now? J. Alzheimer's Dis. 4 (2002) 375–398.
[49] A.J. Anderson, J.H. Su, C.W. Cotman, DNA damage and apoptosis in Alzheimer's disease: colocalization with c-Jun immunoreactivity, relationship to brain area, and effect of postmortem delay, J. Neurosci. 16 (1996) 1710–1719.
[50] C.W. Cotman, J.H. Su, Mechanisms of neuronal death in Alzheimer's disease, Brain Pathol. 6 (1996) 493–506.
[51] C. Behl, Apoptosis and Alzheimer's disease, J. Neural Transm. 107 (2000) 1325–1344.
[52] M.A. Smith, P.L. Richey Harris, L.M. Sayre, J.S. Beckman, G. Perry, Widespread peroxynitrite-mediated damage in Alzheimer's disease, J. Neurosci. 17 (1997) 2653–2657.
[53] A.F. Slater, C. Stefan, I. Nobel, D.J. van den Dobbelsteen, S. Orrenius, Signalling mechanisms and oxidative stress in apoptosis, Toxicol. Lett. 82–83 (1995) 149–153.
[54] B.A. Yankner, New clues to Alzheimer's disease: unraveling the roles of amyloid and tau, Nat. Med. 2 (1996) 850–852.
[55] T. Kratzsch, J. Peters, L. Frolich, Etiology and pathogenesis of Alzheimer dementia, Wien Med. Wochenschr. 152 (2002) 72–76.
[56] L. Gasparini, W.J. Netzer, P. Greengard, H. Xu, Does insulin dysfunction play a role in Alzheimer's disease? Trends Pharmacol. Sci. 23 (2002) 288–293.
[57] K. Kobayashi, H. Nakano, M. Hayashi, M. Shimazaki, Y. Fukutani, K. Sasaki, K. Sugimori, Y. Koshino, Association of phosphorylation site of tau protein with neuronal apoptosis in Alzheimer's disease, J. Neurol. Sci. 208 (2003) 17–24.
[58] J.H. Su, A.J. Anderson, B.J. Cummings, C.W. Cotman, Immunohistochemical evidence for apoptosis in Alzheimer's disease, NeuroReport 5 (1994) 2529–2533.
[59] G. Perry, A. Nunomura, P. Lucassen, H. Lassmann, M.A. Smith, Apoptosis and Alzheimer's disease, Science 282 (1998) 1268–1269.
[60] J. Lewis, D.W. Dickson, W.L. Lin, L. Chisholm, A. Corral, G. Jones, S.H. Yen, N. Sahara, L. Skipper, D. Yager, et al., Enhanced neurofibrillary degeneration in transgenic mice expressing mutant tau and APP, Science 293 (2001) 1487–1491.
[61] K. Ishiguro, A. Omori, M. Takamatsu, K. Sato, M. Arioka, T. Uchida, K. Imahori, Phosphorylation sites on tau by tau protein kinase I, a bovine derived kinase generating an epitope of paired helical filaments, Neurosci. Lett. 148 (1992) 202–206.
[62] H.C. Tseng, Y. Zhou, Y. Shen, L.H. Tsai, A survey of Cdk5 activator p35 and p25 levels in Alzheimer's disease brains, FEBS Lett. 523 (2002) 58–62.
[63] J.J. Pei, I. Grundke-Iqbal, K. Iqbal, N. Bogdanovic, B. Winblad, R.F. Cowburn, Accumulation of cyclin-dependent kinase 5 (cdk5) in neurons with early stages of Alzheimer's disease neurofibrillary degeneration, Brain Res. 797 (1998) 267–277.
[64] H.K. Paudel, J. Lew, Z. Ali, J.H. Wang, Brain proline-directed protein kinase phosphorylates tau on sites that are abnormally phosphorylated in tau associated with Alzheimer's paired helical filaments, J. Biol. Chem. 268 (1993) 23512–23518.
[65] M. Hashiguchi, T. Saito, S. Hisanaga, T. Hashiguchi, Truncation of CDK5 activator p35 induces intensive phosphorylation of Ser202/Thr205 of human tau, J. Biol. Chem. 277 (2002) 44525–44530.
[66] T. Town, J. Zolton, R. Shaffner, B. Schnell, R. Crescentini, Y. Wu, J. Zeng, A. DelleDonne, D. Obregon, J. Tan, et al., p35/Cdk5 pathway mediates soluble amyloid-beta peptide-induced tau phosphorylation in vitro, J. Neurosci. Res. 69 (2002) 362–372.
[67] G. Li, A. Faibushevich, B.J. Turunen, S.O. Yoon, G. Georg, M.L. Michaelis, R.T. Dobrowsky, Stabilization of the cyclin-dependent kinase 5 activator, p35, by paclitaxel decreases beta-amyloid toxicity in cortical neurons, J. Neurochem. 84 (2003) 347–362.
[68] A. Tamura, O. Gotoh, K. Sano, Focal cerebral infarction in the rat: I. Operative technique and physiological monitorings for chronic model, No To Shinkei 38 (1986) 747–751.
[69] P.S. Green, J.W. Simpkins, Neuroprotective effects of estrogens: potential mechanisms of action, Int. J. Dev. Neurosci. 18 (2000) 347–358.
[70] P.M. Wise, Estrogens and neuroprotection, Trends Endocrinol. Metab. 13 (2002) 229–230.
[71] D.W. Choi, Ischemia-induced neuronal apoptosis, Curr. Opin. Neurobiol. 6 (1996) 667–672.
[72] S. Love, Oxidative stress in brain ischemia, Brain Pathol. 9 (1999) 119–131.
[73] H. Patzke, L.H. Tsai, Calpain-mediated cleavage of the cyclin-dependent kinase-5 activator p39 to p29, J. Biol. Chem. 277 (2002) 8054–8060.
[74] M.S. Lee, L.H. Tsai, Cdk5: one of the links between senile plaques and neurofibrillary tangles? J. Alzheimer's Dis. 5 (2003) 127–137.